

Catalytic asymmetric synthesis of cannabinoids and menthol from neral

<https://doi.org/10.1038/s41586-023-05747-9>

Received: 20 August 2022

Accepted: 20 January 2023

Published online: 1 March 2023

Open access

 Check for updates

Joyce A. A. Grimm¹, Hui Zhou^{1,3}, Roberta Properzi^{1,3}, Markus Leutzsch¹, Giovanni Bistoni², Johanna Nienhaus¹ & Benjamin List^{1✉}

The selective conversion of natural or synthetic neral to (1*R*,6*S*)-*trans*-isopiperitenol would enable and expedite sustainable routes to menthol^{1,2} and cannabinoids^{3–5}. However, this reaction has been considered impossible because its product is more reactive to the required acid catalysts than its starting material, resulting in several side products^{6–9}. We now show that an unsymmetric, strong and confined chiral acid, a highly fluorinated imino-imidodiphosphate, catalyses this process with excellent efficiency and selectivity. Expanding the method to other α,β -unsaturated aldehydes could enable access to new cannabinoids and menthol derivatives not readily accessible previously. Mechanistic studies suggest that the confined catalyst accomplishes this reaction by binding the product in an unreactive conformation, thereby preventing its decomposition. We also show how (1*R*,6*S*)-*trans*-isopiperitenol can be readily converted to pharmaceutically useful cannabinoids and menthol, each in the shortest and most atom-economic routes so far.

The asymmetric cyclization of neral to isopiperitenol constitutes an equally attractive and challenging problem for chemists. Although (1*S*,6*R*)-*trans*-isopiperitenol occurs in nature, access to its enantiomer the non-natural (1*R*,6*S*)-*trans*-isopiperitenol would enable extremely short routes to (–)-menthol^{1,2} and several cannabinoids^{3–5}. The growing market volume for synthetic (–)-menthol, which is used in a multitude of consumer products, encompasses hundreds of millions of US dollars. It is used primarily as a cooling and refreshing agent, because menthol is a chemical agonist of the cold-sensitive TRPM8 channel¹⁰. Similarly, several cannabinoids, such as Δ^9 -tetrahydrocannabinol (Δ^9 -THC) and cannabidiol (CBD), are approved for the treatment of side effects in cancer therapy and show promise against several ailments^{11,12}. Cannabinoids target the two G-protein-coupled cannabinoid receptors CB1 and CB2 (refs. ^{13,14}). There is increasing demand for cannabinoids, accompanying the current global trend of legalization for medical and recreational use. Consequently, ever more efficient, industrially applicable routes towards their synthesis are sought, ideally circumventing tedious extraction processes from plants. An elegant and high-yielding approach to cannabinoids uses enantioenriched monoterpene derivatives such as *p*-mentha-2,8-dien-1-ol¹⁵ or *trans*-isopiperitenol^{3,4}. However, access to these terpene building blocks, especially isopiperitenol, requires several steps starting from already enantioenriched natural products^{3,16,17}.

Despite early efforts in the late nineteenth century on the conversion of neral to isopiperitenol from Verley¹⁸ and Semmler¹⁹, it took nearly 100 years to fully uncover its complexity^{6–9}. Under acidic conditions, the cyclization of neral follows a stepwise Prins-like mechanism and initially gives rise to isopiperitenol. However, isopiperitenol, a cyclic allylic alcohol, although stable under neutral conditions, is only metastable even under weakly acidic conditions and is prone to elimination of water, giving complex mixtures of cyclic trienes and aromatic compounds

(Fig. 1). Further side reactions that have been characterized include double-bond isomerizations and, in aqueous media, the re-addition of water furnishing different alcohols. Even though a variety of reaction conditions has previously been evaluated in depth, isopiperitenol can be isolated in only low yields making it merely a reaction intermediate. In the meantime, significant progress has been made towards catalytic asymmetric intramolecular carbonyl-ene and Prins cyclizations of olefinic carbonyl compounds^{20–23}.

For example, we have contributed a highly enantioselective Brønsted acid-catalysed carbonyl-ene cyclization²¹, proceeding via a Prins mechanism, to give five-membered ring products. However, the reactivity towards six-membered rings is insufficient and α,β -unsaturated aldehydes are not investigated in this study. Very recently, the Jacobsen group reported intramolecular Prins-type cyclizations of α,β -unsaturated aldehydes applying cooperative hydrogen-bond-donor catalysis²³. This system seems to be limited to aryl-substituted substrates, and β,β -dialkyl aldehydes such as neral are absent in this report. Inspired by a long-standing interest in the chemistry of citral and encouraged by our previous studies on confinement-controlled reactivity, for example in single aldolizations of acetaldehyde enolates²⁴ and conformationally induced Nazarov cyclizations²⁵, we became interested in the ‘neral to isopiperitenol dilemma’ (Fig. 1). We expected a member of our readily tunable confined Brønsted acid catalyst portfolio to provide sufficient reactivity and enantioselectivity, enabling the smooth asymmetric cyclization of the small and unengineered neral substrate, while simultaneously hoping that enzyme-like confinement effects could prevent product decomposition. Here, we report the development of a new type of unsymmetric and highly fluorinated confined acid that converts neral to (1*R*,6*S*)-*trans*-isopiperitenol, providing asymmetric access to five useful cannabinoids, as well as to menthol and piperitol, each in the shortest and most atom-economic route reported so far.

¹Max-Planck-Institut für Kohlenforschung, Mülheim an der Ruhr, Germany. ²Department of Chemistry, Biology and Biotechnology, University of Perugia, Perugia, Italy. ³These authors contributed equally: Hui Zhou, Roberta Properzi. ✉e-mail: list@kofo.mpg.de

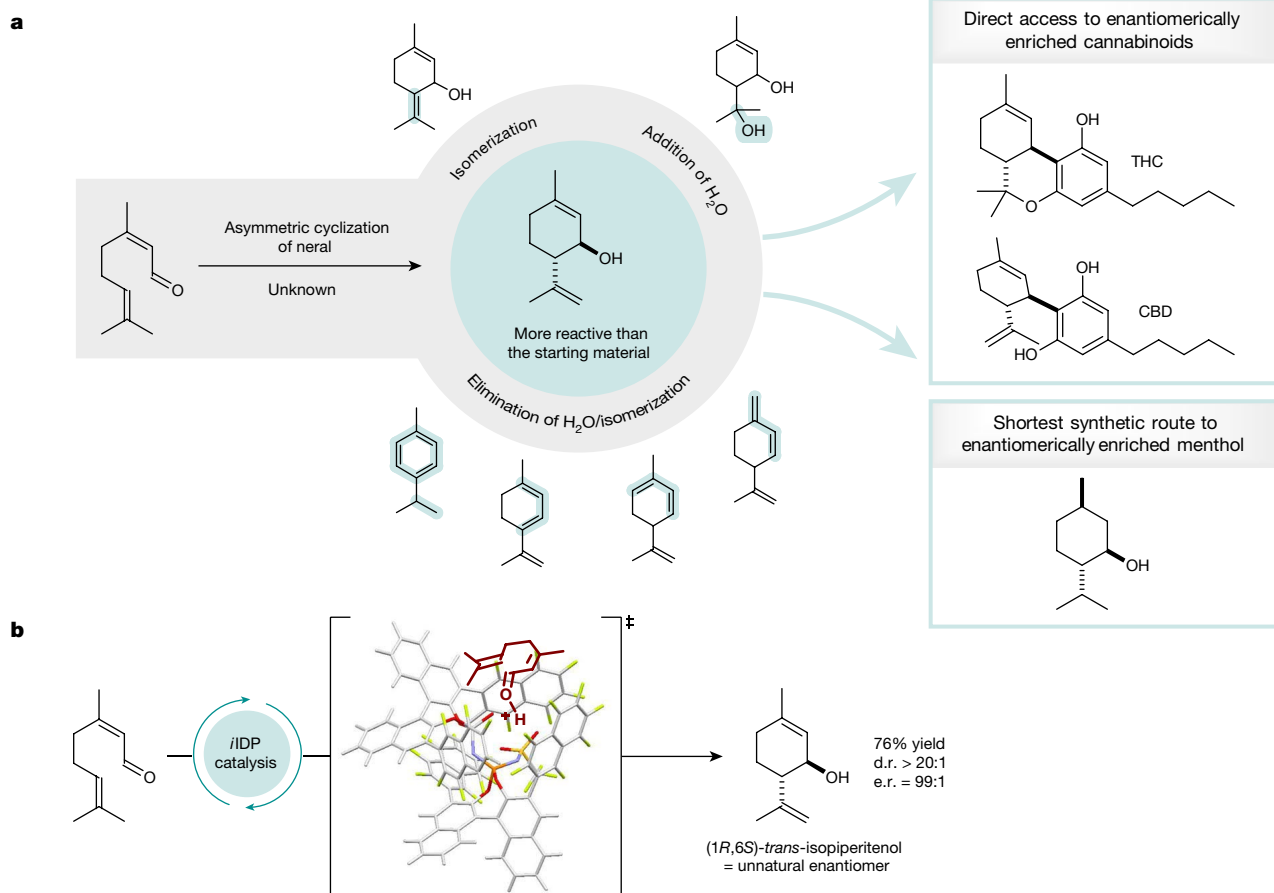


Fig. 1 | Brønsted acid-catalysed cyclization of neral to (1R,6S)-*trans*-isopiperitenol. a, Selectivity problems in the cyclization of neral named the ‘neral to isopiperitenol dilemma’ and isopiperitenol as valuable chiral pool

material in the synthesis of cannabinoids and menthol. **b**, The first asymmetric, selective cyclization of neral to isopiperitenol under confined Brønsted acid catalysis.

At the onset, several mineral and organic achiral Brønsted acids covering a broad pK_a range were tested in the targeted reaction (Supplementary Information). Consistent with previous reports^{6–9}, activation of neral (**1**) depends strongly on the acidity of the catalyst. Whereas mild acids barely show conversion, stronger acids readily activate the substrate. However, this reactivity is usually accompanied by the fast decomposition of isopiperitenol (**2**) leading to an unselective reaction.

The ideal acid catalyst required for this transformation therefore needs to reach a certain pK_a threshold to activate aldehyde **1**, while suppressing the decomposition of **2**. We exemplarily confirmed the higher reactivity of isopiperitenol versus neral with achiral acid **3** ($pK_a = 5.8$, MeCN) using ¹H nuclear magnetic resonance (NMR) reaction monitoring (Fig. 2). Using acid **3**, neral (**1**) remained mostly unreacted (conversion less than 10%) and isopiperitenol (**2**) was decomposed by almost half in 20 h, notably illustrating the challenge at hand. Comparing the readily tunable confined Brønsted acid catalysts **4–6** shed light on the significance of confinement as well as the inner-core architecture towards catalysing the targeted cyclization (Fig. 2). Indeed, we find that not only is a certain acidity required to achieve a balance between the activation of aldehyde **1** and the decomposition of allylic alcohol **2**, but so too is a non- C_2 -symmetric inner core. Accordingly, imino-imidodiphosphates (iIDP), featuring a bifunctional inner-core system with an acidic P=NHTf moiety and a basic P=O moiety, combine excellent reactivity and selectivity for the cyclization of neral (**1**) to isopiperitenol (**2**). We were intrigued to find that best results were obtained with highly fluorinated iIDP catalyst **5**, which furnishes (1R,6S)-*trans*-isopiperitenol in good yield (77%) and excellent diastereo- and enantioselectivity (d.r. > 20:1; e.r. = 99:1) (Fig. 2).

The cyclization of neral can be performed easily on a multigram scale (>4 g, 35 mmol) without any loss of selectivity or yield (Fig. 3). It is noteworthy that catalyst **5** can be recovered in excellent yield (95%) and re-used in further cyclization reactions (Supplementary Information).

Enantiomerically enriched (1R,6S)-*trans*-isopiperitenol (**2**) enables direct access to menthol, piperitol and cannabinoids. Indeed, exhaustive hydrogenation of (1R,6S)-*trans*-isopiperitenol (**2**) using 10 mol% of Lindlar’s catalyst provides 88% yield of a mixture of enantioenriched menthol isomers, in which (–)-menthol (**7**) (68%) and (–)-isomenthol (**8**) (26%) are the main products. Although separation of the isomeric menthol mixtures on a laboratory scale is tedious, purification on an industrial scale routinely involves distillation and subsequent crystallization^{26,27}. It should be noted that despite the long history of technical menthol syntheses, which has provided several highly efficient routes to the stereochemically pure product²⁶, our two-step synthesis starting from easily accessible neral (**1**) is perfectly atom-economic and presents the shortest route reported so far. Moreover, we found that selective hydrogenation of the external double bond using Wilkinson’s catalyst furnishes piperitol (**9**) in excellent yield. Piperitol has potential as a surfactant and odorant because of its medium strength herbal scent and antimicrobial activity²⁸.

Early reports from Dethe³ and Mechoulam⁴ demonstrated the promising applicability of isopiperitenol in Lewis acid-catalysed Friedel–Crafts reactions with resorcinols furnishing cannabinoids. However, the commonly used Lewis acid $BF_3 \cdot Et_2O$, in our hands, although showing high reactivity, typically gives uncertain and unselective reaction profiles resulting in tedious purifications and low yields. Focusing our effort on more reliable and selective methods, we investigated

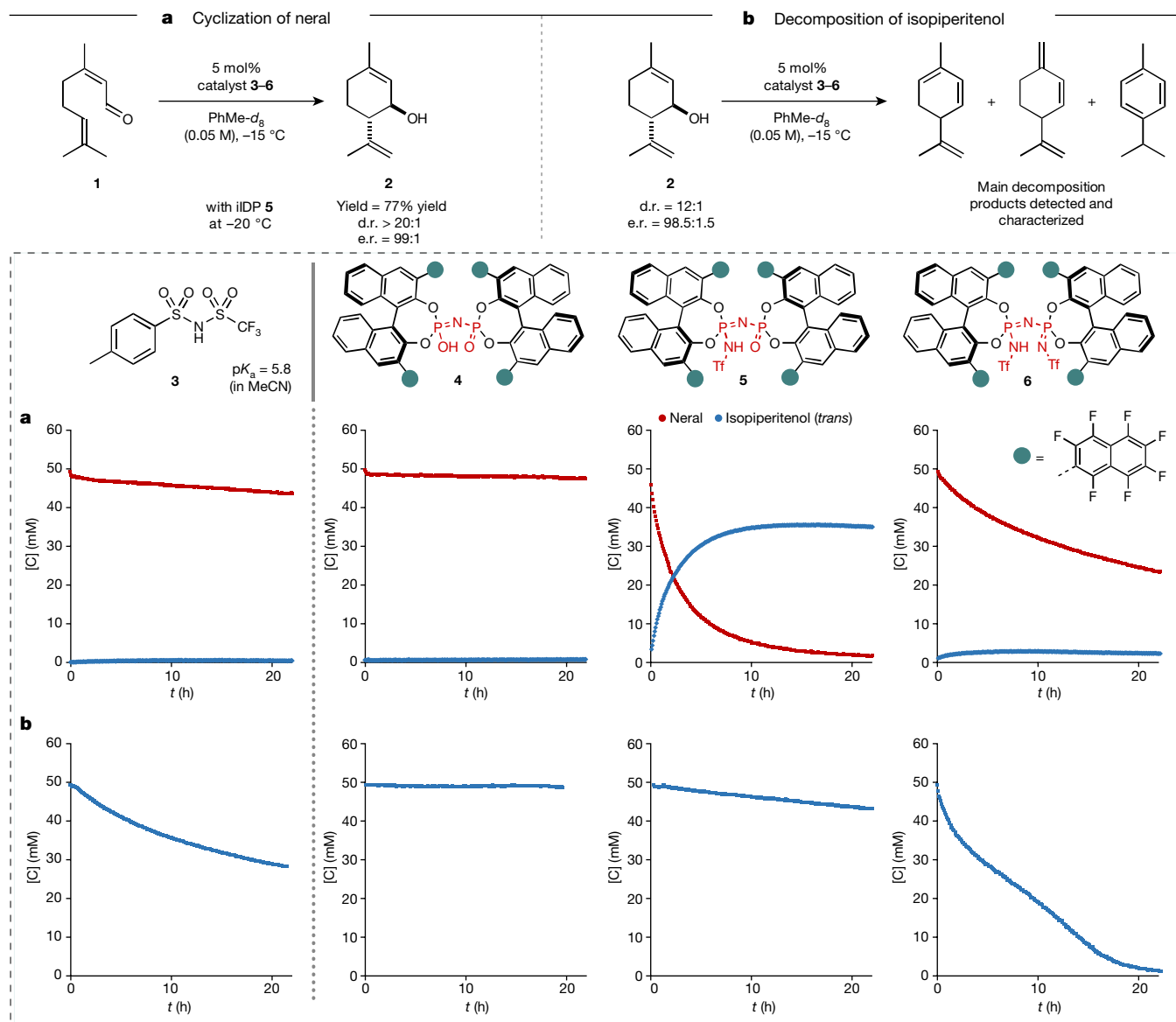


Fig. 2 Comparison of different achiral and chiral Brønsted acids **3-6** in the formation and decomposition of isopiperitenol (**2**). **a, b**, Four different catalysts were used for ^1H NMR reaction monitoring of the cyclization of neral (**a**) and the reaction of isopiperitenol to undesired side products (**b**) under

optimized reaction conditions. d.r. and e.r. were determined by gas chromatography (GC) analysis. The shown decomposition products only represent the main side products characterized by ^1H NMR spectroscopy.

catalysts of varying acidity to selectively obtain different types of cannabinoid. Remarkably, direct access to CBD (**10**) from isopiperitenol (**2**) and olivetol (**12a**) was provided in 35% yield under mild conditions using TsOH·H₂O as catalyst (Fig. 3). It is noteworthy that no further reaction of product **10** to the corresponding tetrahydrocannabinols was observed. These mild conditions were not suitable for the synthesis of ester **11** because resorcinol **12b** proved to be insufficiently reactive in the Friedel–Crafts reaction. Fortunately, using BF₃·Et₂O as a catalyst readily delivered the desired CBD derivative **11** in 61% yield. The most famous Δ^9 -isomer of THC (**13**) could reliably be obtained in 45% yield by employing triflimide as the catalyst in the presence of an excess of triethylsilane. Under these Lewis acidic conditions, isomerization to the thermodynamically more stable Δ^8 -THC (**14**) product was observed only after significantly longer reaction times. Indeed, Δ^8 -THC (**14**) and its pharmaceutically relevant derivative **15** could be obtained from the reaction of isopiperitenol (**2**) and either olivetol (**12a**) or 5-(1,1-dimethylheptyl)resorcinol (**12c**) at ambient temperature, by employing 20 mol% trimethylsilyl triflate as the catalyst. To explore

the generality of our new method, we investigated the cyclization of further α,β -unsaturated aldehydes. Novel cyclic, allylic alcohols **16-24** were obtained in good to excellent yield using optimal iDP catalyst **5** with similarly superb enantioselectivity (e.r. > 98:2). Although elongation of the β -side chain is well tolerated, increased steric demand leads to a loss of diastereoselectivity (**18**, d.r. = 10:1). Noteworthy, the cyclohexyl group in product **24**, which is located in close proximity to the active side of the catalyst and actively engages in the reaction, slows the reaction but excellent levels of enantio- and diastereoselectivity are maintained.

To elucidate the mechanism of the cyclization of neral to isopiperitenol and the reasons for the remarkably high selectivity exerted by privileged iDP catalyst **5**, NMR investigations including deuterium-labelling, as well as computational studies were conducted. First, time normalization analysis following the report from Burés^{29,30} confirmed a first-order reaction in iDP catalyst **5** for both the catalytic cyclization of neral (**1**) (Fig. 4a) and the decomposition of product **2** (Supplementary Information).

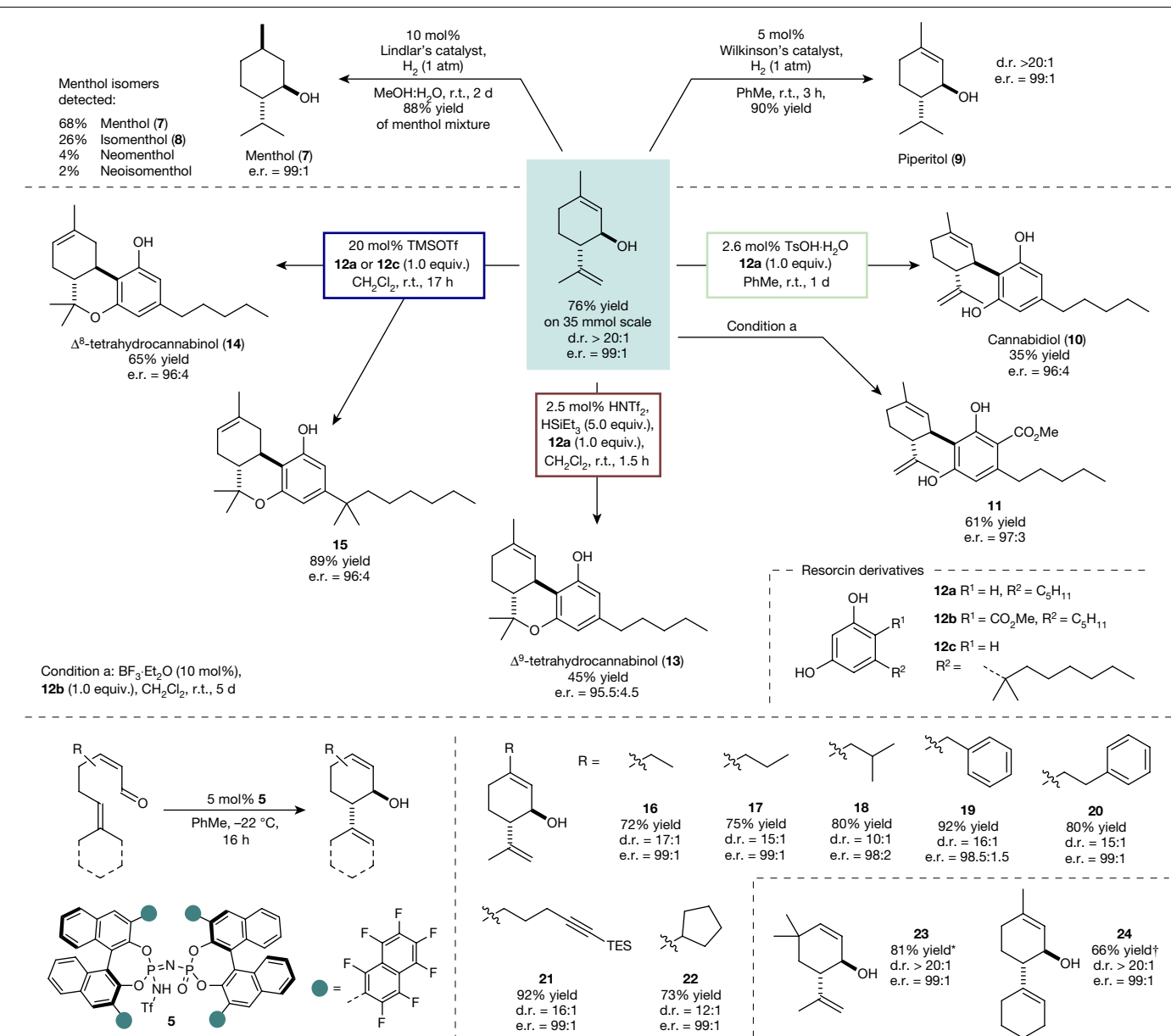


Fig. 3 | Isopiperitenol as a valuable, chiral material in the syntheses of menthol, piperitol and cannabinoids. Hydrogenation reactions to **7** and **9** were performed on 1.0 mmol scale. Reactions to the cannabinoids were performed using an excess of isopiperitenol (1.1–1.5 equiv.). Isolated yields after chromatographic purification. d.r. and e.r. were determined by high-performance liquid chromatography or GC analysis. For the substrate

scope of the asymmetric catalytic cyclization of α,β -unsaturated aldehydes, reactions were performed on a 0.25 mmol scale with **iIDP 5**. Only the main *trans*-diastereoisomer is depicted. d.r. and e.r. were determined by GC analysis. TMSOTf, trimethylsilyl triflate. *Reaction was performed on a 0.025 mmol scale and yield was determined by ¹H NMR spectroscopy using mesitylene as internal standard. †Reaction stirred for 24 h. TMSOTf.

Notably, the reaction order studies showed a decrease in reaction rate over time, suggesting either catalyst decomposition or product inhibition. Two different NMR experiments³¹, independently confirm the stability of the catalyst under the reaction conditions and show a strong inhibition of the reaction by the product (Fig. 4b), reminiscent of competitive inhibition observed with enzymes. At this point, we speculated that the strong interaction of confined catalyst **5** with product **2** might contribute to the peculiar selectivity of our reaction. Indeed, subsequent ¹³C NMR investigations of equimolar mixtures of neral or isopiperitenol with catalyst **5** showed significant shifts of aldehyde and alcohol peaks, suggesting interactions of both moieties with the catalyst (Supplementary Information). Second, we found that in contrast to neral, its double-bond isomer geranial is unreactive under the reaction conditions.

In addition, no notable double-bond isomerization occurred and yield and selectivity remain excellent from neral/geranial mixtures (Supplementary Information). Third, in contrast to our previous report²¹, covalent adducts were not observed by NMR or by mass spectrometry. Last, a deuterium-labelling experiment was conducted to gain insights into the nature of the cyclization reaction (stepwise versus concerted). Accordingly, deuterium-labelled neral **25** was synthesized and deuterium incorporation was found to be 85% at C-8 and 15% at C-9. In case of a concerted carbonyl-ene mechanism, abstraction of a deuterium from C-8 would be required. By contrast, a stepwise process, proceeding via a tertiary cation, could lead to abstraction of either a proton or a deuterium, potentially affected by a kinetic isotope effect. Performing the cyclization reaction using substrate **25**, the corresponding allylic alcohols **26** and **27** were obtained in 63% NMR yield at a ratio

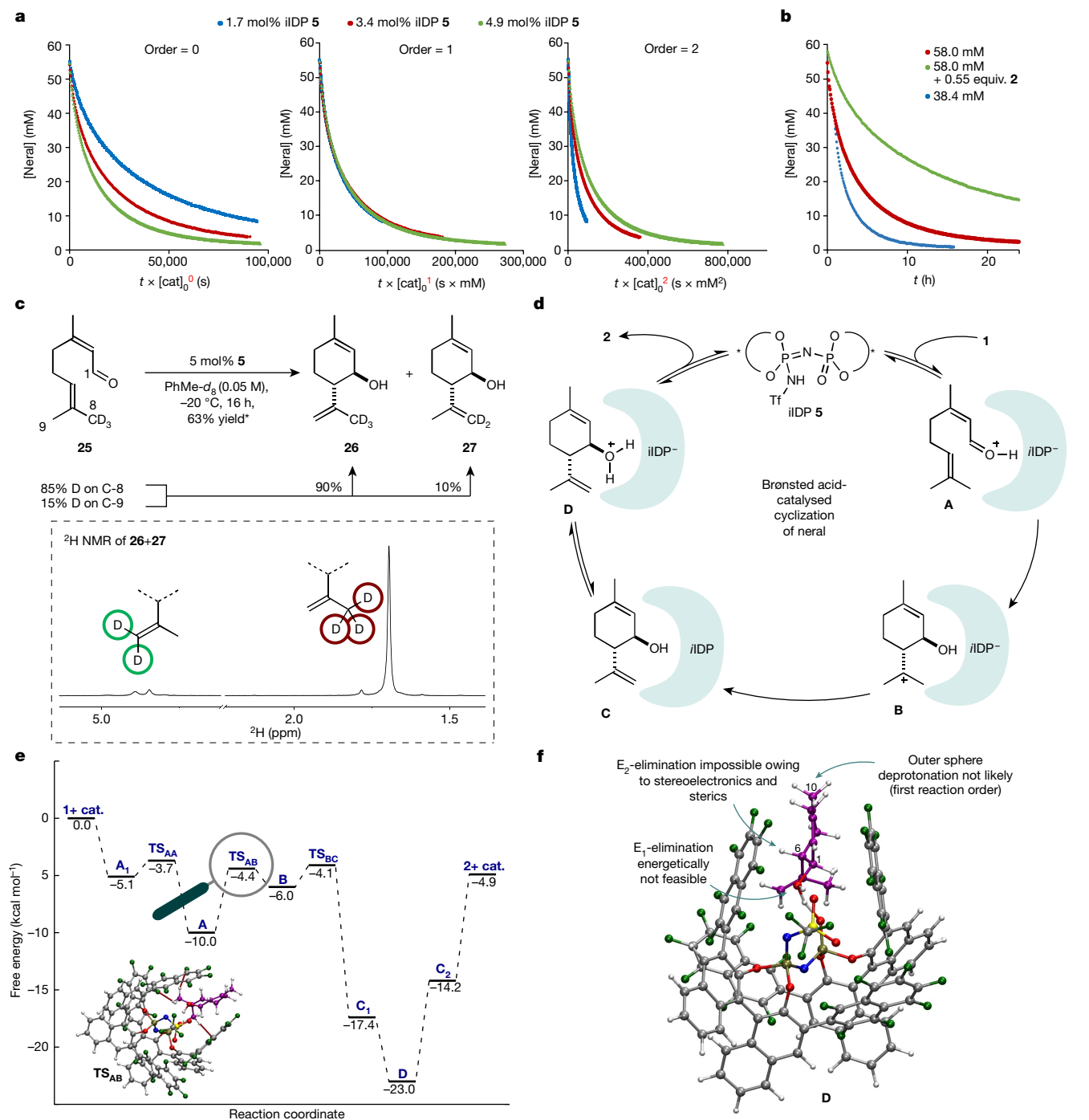


Fig. 4 | Mechanistic studies. **a**, ^1H NMR reaction monitoring to determine the reaction order in catalyst following Burés' method²⁹. **b**, Temporal ^1H NMR concentration profiles³¹ of the reaction under different conditions. The rate differences show strong product inhibition in the cyclization reaction. **c**, Top, deuterium-labelled experiments with 85% C-8 labelled substrate **25**. *The yield is determined by ^1H NMR spectroscopy using mesitylene as an internal standard and is calculated on the basis of neral present in the sample (*Z:E*

of 90:10. On the basis of these findings, a concerted mechanism seemed less probable (Fig. 4c). Because the ratio of products **26** and **27** reflects the starting material composition, both a stepwise and a highly asynchronous concerted pathway are plausible. On the basis of these studies and previous reports from our group^{21,32}, the following catalytic cycle is proposed (Fig. 4d). After initial protonation of the substrate, ion pair **A** is formed. Diastereo- and enantioselectivity determining C–C bond

formation then takes place in a stepwise fashion via structure **B**, which after deprotonation leads to catalyst/product complex **C**. Either this complex or ion pair **D** seem to be the resting state of the catalytic cycle and responsible for the observed strong product inhibition. Finally, decomplexation should provide product **2** and regenerate the catalyst. To validate our proposed catalytic cycle and to clarify the nature of the reaction mechanism (stepwise versus concerted) as well as

the origin of selectivity, computational studies were conducted. The reaction profile at the M062X/def2-TZVP +C-PCM-(toluene) level of theory is shown in Fig. 4e. Interaction of the substrate with the catalyst in reactant complex **A**₁ leads to facile protonation of **1** via transition state TS_{AA}. An ion pair structure consisting of the protonated substrate and iIDP⁻ (**A**) is then formed. Subsequently, the reaction follows a stepwise cyclization (TS_{AB})/deprotonation (TS_{BC}) pathway, proceeding through a highly reactive carbocationic intermediate (**B**) and finally delivering product complex **C**. The product catalyst complexes C₁ (OH-acid) and C₂ (NH-acid) differ only in the position of the acidic proton of iIDP, respectively (Supplementary Information). Interaction of the product with the catalyst in this complex leads to the formation of a stable ion pair between the alcohol protonated product and the iIDP anion (**D**). This computational result is consistent with the experimentally observed product inhibition. Concerning the selectivity of the transformation, the energy difference of the competing cyclization transition states (TS_{AB}) for each of the *trans*-products ($\Delta\Delta G^\ddagger$) is 3.6 kcal mol⁻¹, which is consistent with the high degree of selectivity observed experimentally. We also carried out an analysis of key non-covalent interactions operating in these transition states to elucidate the stereocontrolling factors of this transformation, using dispersion-corrected density functional theory in conjunction with the NCI tool (Supplementary Information). Our analysis showed that the most stable transition state is highly stabilized by dispersion forces. In particular, TS_{AB} features three close C–H...F contacts (Fig. 4e), which contribute significantly to its stability.

A fascinating explanation for the unusual preference of our confined acid catalyst to selectively process **1** rather than its normally more reactive reaction product **2** arises. By non-covalently binding, but not rapidly converting isopiperitenol further, its typically observed acid-mediated decomposition is prevented. In other words, isopiperitenol is a 'substrate' for our enzyme-like catalyst but only towards its protonation and not its decomposition. Computed structure **D** (Fig. 4f), showing the protonated product in the cavity of the catalyst anion, also shows how this is accomplished. A potential E2-elimination by abstracting proton H-6 in this lowest energy conformation is stereoelectronically hampered because of an unfavourable orbital alignment and the inaccessibility of this proton to the active site of the catalyst. Furthermore, an alternative E1-pathway is energetically challenged as suggested by initial calculations (Supplementary Information). A hypothetical outer sphere deprotonation of H-10 by another catalyst also seems to be improbable because the decomposition follows first-order reaction kinetics. Therefore, we believe that the confined active site of our catalyst protects product **2** by stereoelectronically, sterically and energetically disfavoring its decomposition. The methods presented here may facilitate the synthesis of menthol and aid the production of cannabinoids starting from cheap and readily available non-chiral materials. We anticipate use of the concepts advanced here in the development of other challenging transformations.

Online content

Any methods, additional references, Nature Portfolio reporting summaries, source data, extended data, supplementary information, acknowledgements, peer review information; details of author contributions and competing interests; and statements of data and code availability are available at <https://doi.org/10.1038/s41586-023-05747-9>.

1. Van Dyk, M. S., Van Rensburg, E. & Moleleki, N. Hydroxylation of (+)-limonene, (–)- α -pinene and (–)- β -pinene by a *Hormonema* sp. *Biotechnol. Lett.* **20**, 431–436 (1998).
2. Selifonov, S. A. Methods for making (–)-menthol and oxygenated menthane compounds. WO 2004/013339 A1 (2004).

3. Dethle, D. H., Erande, R. D., Mahapatra, S., Das, S. & Kumar, B. V. Protecting group free enantiospecific total syntheses of structurally diverse natural products of the tetrahydrocannabinoid family. *Chem. Commun. (Camb)* **51**, 2871–2873 (2015).
4. Hanus, L. O. et al. Enantiomeric cannabidiol derivatives: synthesis and binding to cannabinoid receptors. *Org. Biomol. Chem.* **3**, 1116–1125 (2005).
5. Mechoulam, R. et al. Fluorinated CBD compounds, compositions and uses thereof. WO 2017/008136 A1 (2017).
6. Horiuchi, R., Otsuki, H. & Okuda, O. Constitution of two new terpenes, menogene and menogene (C10H16 and C10H14) – the mechanism of cyclisation of citronellal and citral. *Bull. Chem. Soc. Jpn* **14**, 501–507 (1939).
7. Price, C. C. & Dickman, M. L. Kinetics of the acid-catalyzed cyclization of citral and citronellal. *Ind. Eng. Chem.* **40**, 257–261 (1948).
8. Clark, B. C., Powell, C. C. & Radford, T. The acid catalyzed cyclization of citral. *Tetrahedron* **33**, 2187–2191 (1977).
9. Peacock, V. E. & Kuneman, D. W. Inhibition of the formation of α -*p*-dimethylstyrene and *p*-cymen-8-ol in a carbonated citral-containing beverage system. *J. Agric. Food Chem.* **33**, 330–335 (1985).
10. Voets, T. et al. The principle of temperature-dependent gating in cold- and heat-sensitive TRP channels. *Nature* **430**, 748–754 (2004).
11. Grotenhermen, F. Pharmacology of cannabinoids. *Neuroendocrinol. Lett.* **25**, 14–23 (2004).
12. Whiting, P. F. et al. Cannabinoids for medical use. *JAMA* **313**, 2456–2473 (2015).
13. Hua, T. et al. Crystal structures of agonist-bound human cannabinoid receptor CB1. *Nature* **547**, 468–471 (2017).
14. Hua, T. et al. Activation and signaling mechanism revealed by cannabinoid receptor–Gi complex structures. *Cell* **180**, 655–665 (2020).
15. Razdan, R. K., Dalzell, H. C. & Handrick, R. G. Hashish. A simple one-step synthesis of (–)- Δ^9 -tetrahydrocannabinol (THC) from *p*-mentha-2,8-dien-1-ol and olivetol. *J. Am. Chem. Soc.* **96**, 5860–5865 (1974).
16. Guillon, J., Rioult, J.-P. & Robba, M. New synthesis of isopiperitenol, previously isolated from species of *Cymbopogon*. *Flavour Fragr. J.* **15**, 223–224 (2000).
17. Golliher, A. E. et al. Using (+)-carvone to access novel derivatives of (+)-*ent*-cannabidiol: the first asymmetric syntheses of (+)-*ent*-CBDP and (+)-*ent*-CBDV. *Tetrahedron Lett.* **67**, 152891 (2021).
18. Verley, M. A. Action des acides sur le citral. *Bull. Soc. Chim. Fr.* **21**, 409–418 (1899).
19. Semmler, F. W. Über olefinische Bestandteile ätherischer Öle. *Berichte der deutschen chemischen Gesellschaft* **24**, 201–211 (1891).
20. Grachan, M. L., Tudge, M. T. & Jacobsen, E. N. Enantioselective catalytic carbonyl-ene cyclization reactions. *Angew. Chem. Int. Ed. Engl.* **47**, 1469–1472 (2008).
21. Liu, L. et al. Confined acid-catalyzed asymmetric carbonyl-ene cyclization. *J. Am. Chem. Soc.* **137**, 13268–13271 (2015).
22. Ishihara, H., Huang, J., Mochizuki, T., Hatano, M. & Ishihara, K. Enantio- and diastereoselective carbonyl-ene cyclization–acetalization tandem reaction catalyzed by tris(pentafluorophenyl)borane-assisted chiral phosphoric acids. *ACS Catal.* **11**, 6121–6127 (2021).
23. Kutateladze, D. A. & Jacobsen, E. N. Cooperative hydrogen-bond-donor catalysis with hydrogen chloride enables highly enantioselective Prins cyclization reactions. *J. Am. Chem. Soc.* **143**, 20077–20083 (2021).
24. Schreyer, L. et al. Confined acids catalyze asymmetric single aldolizations of acetaldehyde enolates. *Science* **362**, 216–219 (2018).
25. Ouyang, J., Kennemur, J. L., De, C. K., Farès, C. & List, B. Strong and confined acids enable a catalytic asymmetric Nazarov cyclization of simple divinyl ketones. *J. Am. Chem. Soc.* **141**, 3414–3418 (2019).
26. Dylong, D., Hausoul, P. J. C., Palkovits, R. & Eisenacher, M. Synthesis of (–)-menthol: industrial synthesis routes and recent development. *Flavour Fragr. J.* **37**, 195–209 (2022).
27. Brink, R., Heuer, L., Kuhlmann, S., Mechelhoff, M. & Pfohl, O. Separation of isomeric menthol compounds. US9,024,079 B2 (2015).
28. Cornnell, R. J. et al. Antimicrobial composition. US2015/0050220 A1 (2015).
29. Burés, J. A simple graphical method to determine the order in catalyst. *Angew. Chem.* **128**, 2068–2071 (2016).
30. Nielsen, C. D. T. & Burés, J. Visual kinetic analysis. *Chem. Sci.* **10**, 348–353 (2019).
31. Baxter, R. D., Sale, D., Engle, K. M., Yu, J.-Q. & Blackmond, D. G. Mechanistic rationalization of unusual kinetics in Pd-catalyzed C–H olefination. *J. Am. Chem. Soc.* **134**, 4600–4606 (2012).
32. Diaz-Oviedo, C. D., Maji, R. & List, B. The catalytic asymmetric intermolecular Prins reaction. *J. Am. Chem. Soc.* **143**, 20598–20604 (2021).

Publisher's note Springer Nature remains neutral with regard to jurisdictional claims in published maps and institutional affiliations.



Open Access This article is licensed under a Creative Commons Attribution 4.0 International License, which permits use, sharing, adaptation, distribution and reproduction in any medium or format, as long as you give appropriate credit to the original author(s) and the source, provide a link to the Creative Commons licence, and indicate if changes were made. The images or other third party material in this article are included in the article's Creative Commons licence, unless indicated otherwise in a credit line to the material. If material is not included in the article's Creative Commons licence and your intended use is not permitted by statutory regulation or exceeds the permitted use, you will need to obtain permission directly from the copyright holder. To view a copy of this licence, visit <http://creativecommons.org/licenses/by/4.0/>.

© The Author(s) 2023

Data availability

The experimental procedures and analytical data supporting the findings of this study are available in the manuscript and its Supplementary Information file. Raw and unprocessed NMR data are available from the corresponding author on reasonable request.

Acknowledgements Generous support from the Max Planck Society, the Deutsche Forschungsgemeinschaft (DFG, German Research Foundation), Leibniz Award to B.L. and under Germany's Excellence Strategy-EXC 2033-390677874-RESOLV, and the European Research Council (ERC, European Union's Horizon 2020 research and innovation program "C-H Acids for Organic Synthesis, CHAOS" Advanced Grant Agreement No. 694228). The authors thank Alexander Zwerschke for synthetic contributions and C. David Diáz-Oviedo for sharing catalysts. We thank Oleg Grossmann for fruitful discussions. We also thank the technicians of our group and the members of our GC, MS, HPLC and NMR service departments, especially Veronika Dietl, Sandra Eichler and Phil Hesse from the GC department, for their excellent service.

Author contributions B.L. designed and oversaw the project. After initial experiments from H.Z., J.A.A.G. developed and optimized the cyclization reaction. J.A.A.G. and J.N. performed the substrate syntheses. J.A.A.G. performed the large-scale reactions of neral, the other

α,β -unsaturated substrates and the hydrogenation experiments. R.P. and H.Z. conducted the synthesis of the cannabinoids. J.A.A.G. and R.P. synthesized the deuterated substrate. M.L. performed the kinetic studies using NMR spectroscopy together with J.A.A.G. and R.P. G.B. performed the computational studies. J.A.A.G., R.P. and B.L. wrote the manuscript. J.A.A.G. and B.L. revised the manuscript.

Funding Open access funding provided by Max Planck Society.

Competing interests A patent on the synthesis of imino-imidodiphosphates (iIDP) catalysts has been filed (patent no. WO 2017/037141 A1, EP 3 138 845 A1). Furthermore, a patent on an improved synthesis of imidodiphosphoryl-derived catalysts using hexachlorophosphazonium salts has been filed (patent no. EP 3 981 775 A1). The authors also filed a patent on the acid-catalysed cyclization of α,β -unsaturated aldehydes and its application in the synthesis of menthol and cannabinoids (patent no. EP 4 023 626 A1).

Additional information

Supplementary information The online version contains supplementary material available at <https://doi.org/10.1038/s41586-023-05747-9>.

Correspondence and requests for materials should be addressed to Benjamin List.

Peer review information *Nature* thanks Spyros Nikas and Thanh C. Ho for their contribution to the peer review of this work.

Reprints and permissions information is available at <http://www.nature.com/reprints>.